

# COLOR SEGMENTATION THROUGH INDEPENDENT ANISOTROPIC DIFFUSION OF COMPLEX CHROMATICITY AND LIGHTNESS

Luca Lucchese and Sanjit K. Mitra

Department of Electrical and Computer Engineering  
University of California at Santa Barbara, CA 93106

## ABSTRACT

This paper presents a new technique based on anisotropic diffusion for segmenting color images. This operation is accomplished through two independent anisotropic diffusion processes: one involving only the chromatic information, conveniently embedded in a complex function, and the other affecting the lightness information. The results of the two diffusions are separately segmented and their combination allows the color image to be eventually partitioned. We report on some experimental results verifying the effectiveness of such a technique.

## 1. INTRODUCTION

Segmentation is an operation of paramount importance in a number of image processing applications. A great deal of techniques have been proposed for both gray-level images [1] and color images [2]. In this paper we present a new segmentation algorithm for color images which is based on anisotropic diffusion [3, 4]. This nonlinear filtering technique shows in fact an extremely interesting property from the point of view of segmentation: the smoothing is selective, being encouraged in homogeneous regions and inhibited across region boundaries. Thus, noise and irrelevant image details can be filtered out, making it easier for a segmentation algorithm to achieve spatial compactness while retaining the edge information. Several researchers have resorted to this tool as a preprocessing step for segmentation algorithms targeted to gray-level images. However, even though diffusion of vector-valued functions, such as color images or multispectral data, has already a solid background, its has been mainly aimed at filtering, denoising, and enhancement [5, 6, 7].

In this paper, we present a clustering-based algorithm for segmentation of color images which extends our previous work by harnessing the attractive property of anisotropic diffusion. In [8], we showed that an effective segmentation scheme consists in splitting chromatic and luminance information, separately clustering them, and finally combining the two results, as opposite to traditional methods which performs clustering directly in 3-D color spaces. The physical rationale supporting this scheme is that hue and saturation are the color features which provide the most useful basis for judging color uniformity, being rather invariant to surface curvature and lighting conditions [9]. Therefore, a chromatic space carrying hue and saturation information should be the first feature space to take into account for color segmentation. On the other hand, regions with low chromatic content should be segmented by using luminance information.

THIS WORK WAS SUPPORTED BY A UNIVERSITY OF CALIFORNIA MICRO GRANT WITH MATCHING SUPPORTS FROM NATIONAL SEMICONDUCTOR CORP., LUCENT TECHNOLOGIES, AND TEKTRONIX CORP.

This strategy is embraced also in our present contribution. With the formalism of phasors, hue and saturation are conveniently represented as a complex chromaticity function which is diffused prior to being clustered and segmented. The scalar lightness information is separately diffused, clustered, and segmented. The combination of the two parallel segmentation processes allows the original color image to be partitioned. We report a few examples which confirm the effectiveness of this technique.

This work has four sections. Section 2 briefly discusses the formats and the vector spaces used in this paper for representing and handling color information. Section 3 details our segmentation technique. Section 4 presents the conclusions.

## 2. COLOR REPRESENTATION

We represent a color image  $\mathbf{C}$  in a vector form as  $\mathbf{C}(\mathbf{x}) = [R(\mathbf{x}) G(\mathbf{x}) B(\mathbf{x})] \in \mathbb{R}^3$ ,  $\mathbf{x} \in \mathbb{R}^2$ , where  $R(\mathbf{x})$ ,  $G(\mathbf{x})$ , and  $B(\mathbf{x})$  are, respectively, the red, green, and blue channels conveniently normalized between 0 and 1. The color image  $\mathbf{C}$  is represented in the CIE XYZ space [9] as  $\mathbf{C}(\mathbf{x}) = [X(\mathbf{x}) Y(\mathbf{x}) Z(\mathbf{x})]$ , whence the two chromatic channels  $u'(\mathbf{x})$  and  $v'(\mathbf{x})$  are derived, respectively, as  $u'(\mathbf{x}) = 4X(\mathbf{x}) / (X(\mathbf{x}) + 15Y(\mathbf{x}) + 3Z(\mathbf{x}))$  and  $v'(\mathbf{x}) = 9Y(\mathbf{x}) / (X(\mathbf{x}) + 15Y(\mathbf{x}) + 3Z(\mathbf{x}))$ . This information may be expressed in a polar form through the hue-angle  $\vartheta(\mathbf{x}) \doteq \arctan((v'(\mathbf{x}) - v'_N) / (u'(\mathbf{x}) - u'_N))$  and the saturation<sup>1</sup>  $\sigma(\mathbf{x}) \doteq ((u'(\mathbf{x}) - u'_N)^2 + (v'(\mathbf{x}) - v'_N)^2)^{1/2}$ , where  $u'_N$  and  $v'_N$  are the values of  $u'$  and  $v'$  of a suitably chosen reference white [9] (in our experiments, we have adopted the coordinates of the standard illuminant  $D_{65}$ :  $u'_N = 0.1978$  and  $v'_N = 0.4683$ ). As an example, Fig. 1 shows<sup>2</sup> the signals  $\vartheta(\mathbf{x})$  and  $\sigma(\mathbf{x})$  relative to the image of the parrots of Fig. 2. With the formalism of phasors, we conveniently represent these chromatic components in the complex plane  $\mathbb{C}$  (see also [10]) as  $\kappa(\mathbf{x}) = \sigma(\mathbf{x}) \exp(j\vartheta(\mathbf{x}))$ . Henceforth,  $\kappa(\mathbf{x})$  will be referred to as the *complex chromaticity*.

The image brightness is encoded through the CIE  $L^*$  lightness signal defined as  $\ell(\mathbf{x}) = 116(Y(\mathbf{x})/Y_N)^{1/3} - 16$  for  $Y(\mathbf{x})/Y_N > 0.008856$  and  $\ell(\mathbf{x}) = 903.3(Y(\mathbf{x})/Y_N)$  for  $Y(\mathbf{x})/Y_N \leq 0.008856$  [9], where  $Y_N$  is the  $Y$  value for the reference white; we have chosen  $Y_N = 1$  (perfect diffuser). Fig. 1 shows the lightness signal  $\ell(\mathbf{x})$  relative to the image of the parrots of Fig. 2.

<sup>1</sup>For convenience, we dropped the scaling factor 13 usually included in the definition of saturation in  $u'v'$  coordinates [9].

<sup>2</sup>Hue is defined over  $[0, 2\pi)$  and is displayed in such a way that 0 corresponds to black and  $2\pi$  to white; similarly, a saturation of value 0 is displayed as black and its maximum value, dependent on the image, is displayed as white.

### 3. SEGMENTATION ALGORITHM

#### 3.1. Anisotropic diffusion of $\kappa(\mathbf{x})$ and $\ell(\mathbf{x})$

The complex chromaticity  $\kappa(\mathbf{x})$  is embedded in a one-parameter family of “derived” images  $\kappa(\mathbf{x}, t)$ , where the parameter  $t \in \mathbb{R}$  can be regarded either as time or as an iteration step; more explicitly, this function reads  $\kappa(\mathbf{x}, t) = \sigma(\mathbf{x}, t) \exp(j\vartheta(\mathbf{x}, t))$ . The anisotropic diffusion of  $\kappa(\mathbf{x}, t)$  is carried out by means of the partial differential equation [3]

$$\frac{\partial}{\partial t} \kappa(\mathbf{x}, t) = \text{div}(c(\mathbf{x}, t) \nabla \kappa(\mathbf{x}, t)), \quad (1)$$

where  $\text{div}$  and  $\nabla \doteq [\frac{\partial}{\partial x} \frac{\partial}{\partial y}]^T$  respectively denote the divergence and the gradient operators, and  $c(\mathbf{x}, t) = f(|\nabla \kappa(\mathbf{x}, t)|)$  is a monotonically decreasing function of the image gradient magnitude (*conductance coefficient*), chosen as  $c(\mathbf{x}, t) = (1 + (|\nabla \kappa(\mathbf{x}, t)|/\gamma_\kappa)^2)^{-1}$  [3]. The gradient of  $\kappa(\mathbf{x}, t)$  (*chromatic gradient*) is given by  $\nabla \kappa(\mathbf{x}, t) = (\nabla \sigma(\mathbf{x}, t) + j\sigma \nabla \vartheta(\mathbf{x}, t)) \exp(j\vartheta(\mathbf{x}, t))$  and its magnitude is  $|\nabla \kappa(\mathbf{x}, t)| = (\|\nabla \sigma(\mathbf{x}, t)\|^2 + \sigma^2(\mathbf{x}, t) \|\nabla \vartheta(\mathbf{x}, t)\|^2)^{1/2}$ . It should be noted that, in the magnitude of the chromatic gradient, variations of hue are correctly weighted by the level of color saturation, in agreement with the fact that hue becomes less important at low saturation. For the numerical implementation of Eq. (1), we have followed the simple discretization scheme provided by Perona and Malik in [3] with  $N_i = 30$  iterations and the *diffusion coefficient*  $\gamma_\kappa$  selected as the 5% of the maximum value<sup>3</sup> of  $|\nabla \kappa(\mathbf{x}, t)|$  at each iteration.

Let  $\kappa_d(\mathbf{x}) \doteq \sigma_d(\mathbf{x}) \exp(j\vartheta_d(\mathbf{x}))$  denote the result of the diffusion process of  $\kappa(\mathbf{x}, t)$  at time  $t = N_i$ . Fig. 1 shows  $\vartheta_d(\mathbf{x})$  and  $\sigma_d(\mathbf{x})$  relative to  $\vartheta(\mathbf{x})$  and  $\sigma(\mathbf{x})$  of the same figure.

A few important observations are in order. First, the formalism of complex phasors that we have adopted to model the chromatic information of images allows us to carry out the diffusion of an intrinsically vector-valued function in a “scalar” fashion, without resorting to *ad hoc* techniques for vector-valued images [5]. Second, the combined diffusion of hue and saturation through  $\kappa(\mathbf{x})$  allows us to bypass the possible numerical instabilities associated with the diffusion of hue alone [11]. Third, the beneficial synergism of hue and saturation components in the diffusion process of Eq. (1), which is the main contribution of this work, may be better appreciated by separating the real and imaginary parts of such an equation. By doing so, we get

$$\begin{cases} \frac{\partial}{\partial t} \sigma = \text{div}(c \nabla \sigma) - c \sigma \|\nabla \vartheta\|^2, \\ \frac{\partial}{\partial t} \vartheta = \text{div}(c \nabla \vartheta) + 2 \left(\frac{c}{\sigma}\right) \nabla^T \sigma \nabla \vartheta, \end{cases} \quad (2)$$

where we have dropped space and time variables for compactness. Based upon the system of coupled diffusion equations in Eq. (2), we can make the following remarks. 1) In a region where hue is almost constant,  $\|\nabla \vartheta\| \simeq 0$ ; hue and saturation therefore tend to diffuse independently and the common conductance coefficient depends only on the saturation gradient information because  $c \simeq f(|\nabla \sigma|)$ . 2) In a region where saturation is almost constant,  $\|\nabla \sigma\| \simeq 0$ ; in this case the conductance coefficient depends on the hue gradient information weighted by saturation since

<sup>3</sup>The hue function  $\vartheta(\mathbf{x})$  takes on values in  $[0, 2\pi)$ ; however, accounting for the circular nature of this quantity, the difference between  $\vartheta_1$  and  $\vartheta_2$  is defined to be  $\vartheta_1 - \vartheta_2 \doteq \min(\Delta\vartheta, 2\pi - \Delta\vartheta)$  where  $\Delta\vartheta \doteq |\vartheta_1 - \vartheta_2|$ .

$c \simeq f(\sigma |\nabla \vartheta|)$ . The hue diffusion depends on saturation information only through the conductance coefficient: the diffusion is inhibited by high saturation values. Instead, the saturation diffusion shows a negative feedback, weighted by saturation itself, with the hue gradient; this means that a hue edge tends to contrast saturation diffusion and that this action is more effective at high levels of saturation. 3) In a region where both hue and saturation are almost constant,  $c \simeq 1$  and the two chromatic components are decoupled and diffuse independently at high rate.

The lightness signal  $\ell(\mathbf{x})$  is diffused with an analogous procedure; the signal is embedded in a one-parameter family of “derived” images  $\ell(\mathbf{x}, t)$  and filtered with Eq. (1) by replacing  $\kappa(\mathbf{x})$  with  $\ell(\mathbf{x})$ . In this case, the value of the diffusion constant  $\gamma_\ell$  is set as the 5% of  $|\nabla \ell(\mathbf{x})|$  at each iteration; the number of iterations is again  $N_i = 30$ . Fig. 1 shows the diffused lightness  $\ell_d(\mathbf{x})$  relative to  $\ell(\mathbf{x})$  of the same figure. The selective smoothing is apparent in all three diffused signals.

#### 3.2. Quantization and clustering

The segmentation of the image  $\mathbf{C}(\mathbf{x})$  is achieved by separately partitioning  $\kappa_d(\mathbf{x})$  and  $\ell_d(\mathbf{x})$ , and by combining the two results. The k-means clustering technique of [8] may be used for both these tasks by conveniently quantizing  $\kappa_d(\mathbf{x})$  and  $\ell_d(\mathbf{x})$ , and representing them in a palettized format. In fact, the diffusion process, in general, produces as many values in  $\vartheta_d(\mathbf{x})$ ,  $\sigma_d(\mathbf{x})$ , and  $\ell_d(\mathbf{x})$  as the product of the image dimensions, and a clustering based on these functions would be overly computationally intensive. We thus proceed as follows. 1) By inverting the transformation relationships reported in Section 2, from  $\vartheta_d(\mathbf{x})$ ,  $\sigma_d(\mathbf{x})$ , and  $\ell_d(\mathbf{x})$  we construct the diffused RGB image  $\mathbf{C}_d(\mathbf{x}) = [R_d(\mathbf{x}) \ G_d(\mathbf{x}) \ B_d(\mathbf{x})]$ . 2) We then quantize  $\mathbf{C}_d(\mathbf{x})$  as  $\mathbf{C}_q(\mathbf{x})$  with  $N_q$  colors (in our implementation,  $N_q = 1024$ ). 3) Finally, we represent the quantized image in a palettized format [8] as  $\mathbf{C}_q(\mathbf{x}) = \{\mathcal{Q}_q(\mathbf{x}), \mathbf{P}_q, \mathcal{W}_q\}$ , where the values taken on by  $\mathcal{Q}_q(\mathbf{x})$  are pointers to a look-up-table  $\mathbf{P}_q = [\kappa_q \ \ell_q]$  (a matrix of size  $N_q \times 2$  with complex entries in the first column and real entries in the second),  $\kappa_q \doteq \sigma_q \exp(j\vartheta_q)$ , and  $\mathcal{W}_q$  is a vector that contains the number of pixels in  $\mathcal{Q}_q(\mathbf{x})$  having the values of  $\mathbf{P}_q$ . The signals  $\kappa_q$  and  $\ell_q$  are then segmented with the algorithm presented in [8] and the results are displayed in last row of Fig. 1.

By combining the segmentations of hue, saturation, and lightness of the last row of Fig. 1, we finally obtained the result shown in Fig. 2. Fig. 2 also reports other examples of segmentation with various images which bear out the effectiveness of our algorithm. On the whole, it should be noted that our technique performs pretty well. However, there exist some problems of oversegmentation in regions affected by highlights and shadows (see the images of the fruits, of the peppers, and of the wall with the door). These limits are due to the fact that our segmentation algorithm is exclusively feature-based. In order to prevent oversegmentation, one should resort to physics-based techniques which account for the physical processes involved in the interaction of light with matter (*e.g.*, see [12] and references therein).

### 4. CONCLUSIONS

We have presented a new technique for color image segmentation. It is based on two independent diffusion processes: one applied to the chromatic information, conveniently embedded in a complex function; the second applied to the lightness information. The results of the two diffusions are separately segmented and their com-

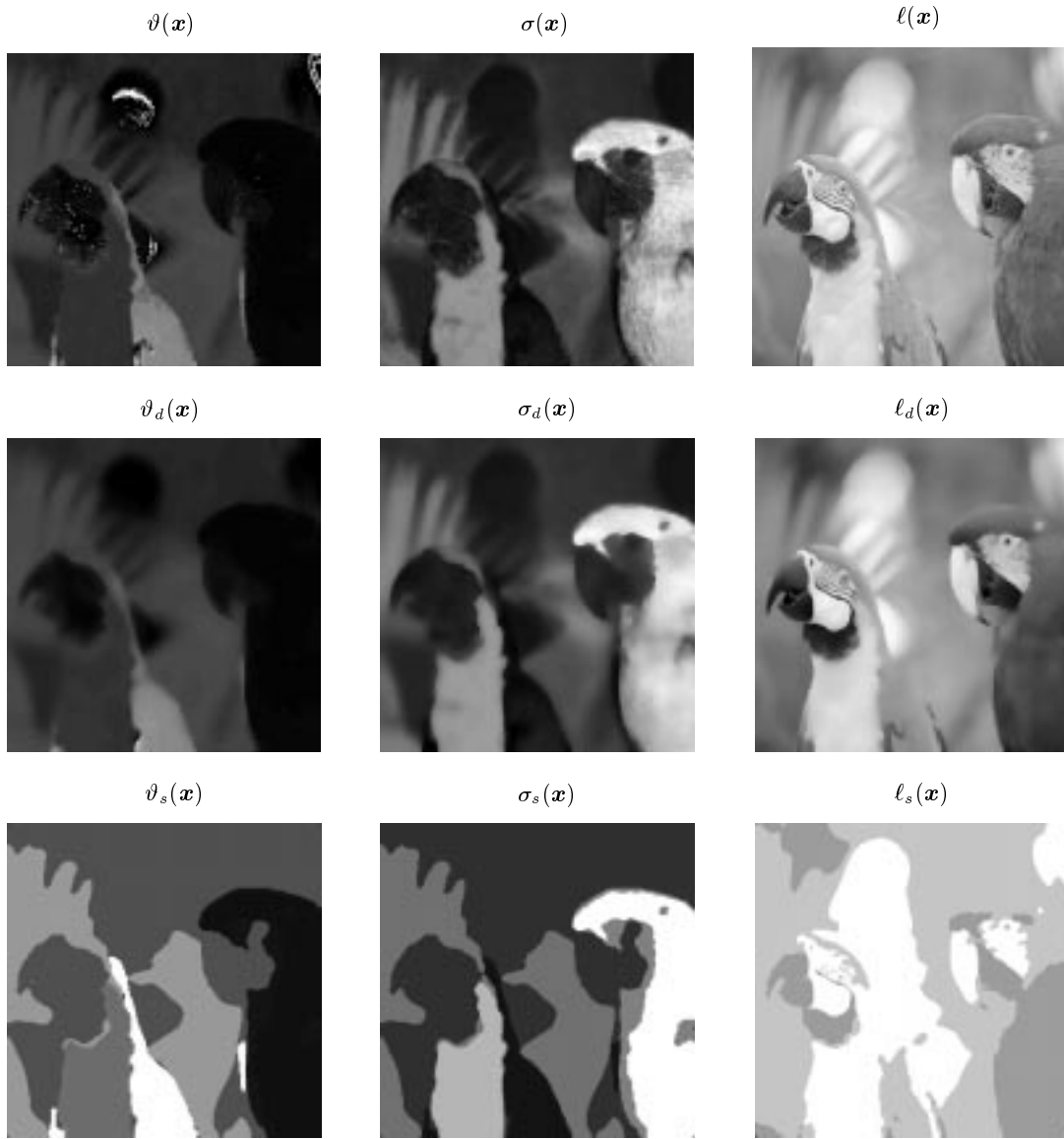


**Fig. 1.** First row: Original hue  $\vartheta(\mathbf{x})$ , saturation  $\sigma(\mathbf{x})$ , and lightness  $\ell(\mathbf{x})$  (from left to right). Second row: Diffused hue  $\vartheta_d(\mathbf{x})$ , saturation  $\sigma_d(\mathbf{x})$ , and lightness  $\ell_d(\mathbf{x})$ . Third row: Segmented hue  $\vartheta_s(\mathbf{x})$ , saturation  $\sigma_s(\mathbf{x})$ , and lightness  $\ell_s(\mathbf{x})$ .

bination allows the color image partitioning. We have reported some examples verifying the effectiveness of our technique. Further details on this segmentation technique can be found in [13].

## 5. REFERENCES

- [1] N.R. Pal and S. K. Pal, "A Review on Image Segmentation Techniques," *Pattern Recognition*, Vol. 26, No. 9, pp. 1277-1294, 1993.
- [2] L. Lucchese and S.K. Mitra, "Advances in Color Image Segmentation," *Proc. of Globecom'99*, Rio de Janeiro, Brazil, Dec. 1999, pp. 2038-2044.
- [3] P. Perona and J. Malik, "Scale Space and Edge Detection Using Anisotropic Diffusion," *IEEE Trans. on PAMI*, Vol. 12, No. 7, pp. 629-639, July 1990.
- [4] B.M. ter Haar Romeny (Ed.), *Geometry-Driven Diffusion in Computer Vision*, Kluwer Academic Publishers, 1994.
- [5] R. Whitaker and G. Gerig, "Vector-valued Diffusion," in *Geometry-Driven Diffusion in Computer Vision*, B.M. ter Haar Romeny (Ed.), pp. 93-134, July 1990.
- [6] G. Sapiro and D.L. Ringach, "Anisotropic Diffusion of Multivalued Images with Application to Color Filtering," *IEEE Trans. on Image Processing*, Vol. 5, No. 11, pp. 1582-1586, Nov. 1996.
- [7] G. Sapiro, "Cromaticity Diffusion," *Proc. of ICIP 2000*, Vancouver, BC, Canada, Sept. 2000, Vol. II, pp. 784-787.
- [8] L. Lucchese and S.K. Mitra, "Unsupervised Segmentation of Color Images Based on  $k$ -means Clustering in the Chromaticity Plane," *Proc. of CBAIVL'99*, Fort Collins, CO, June 1999, pp. 74-78.
- [9] R.W.G. Hunt, *The Reproduction of Colour*, 5<sup>th</sup> Ed., Fountain Press, Kingstone-upon-Thames, UK, 1995.
- [10] A. McCabe, G. West, and T. Caelli, "Filter Techniques for Complex Spatio-Chromatic Image Processing," *Proc. of ICIP98*, Vol. II, pp. 742-746.
- [11] P. Perona, "Orientation Diffusions," *Proc. of IEEE Trans. on Image Processing*, Vol. 7, No. 3, pp. 457-467, Mar. 1998.
- [12] B.A. Maxwell and S.A. Shafer, "Physics-Based Segmentation of Complex Object Using Multiple Hypotheses of Image Formation," *Computer Vision and Image Understanding*, Vol. 65, No. 2, pp. 269-295, Feb. 1997.
- [13] L. Lucchese and S.K. Mitra, "Color Segmentation Based on Separate Anisotropic Diffusion of Chromatic and Achromatic Channels," to appear in *IEE Proceedings: Vision, Image, and Signal Processing*.

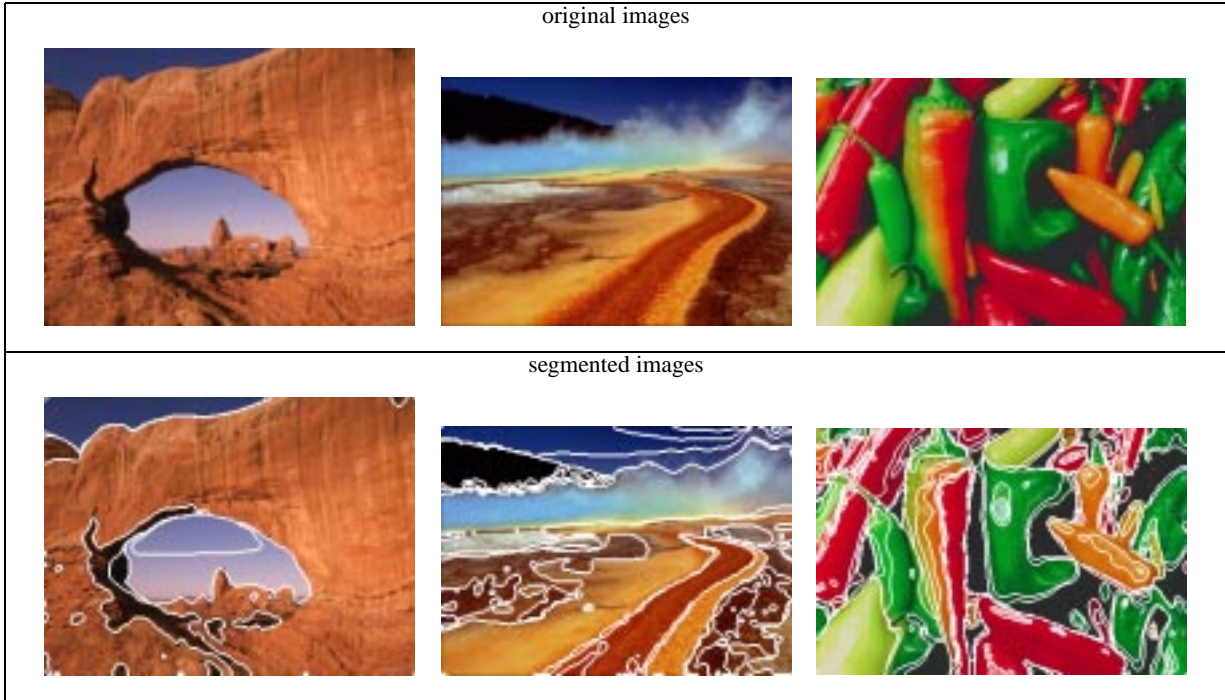
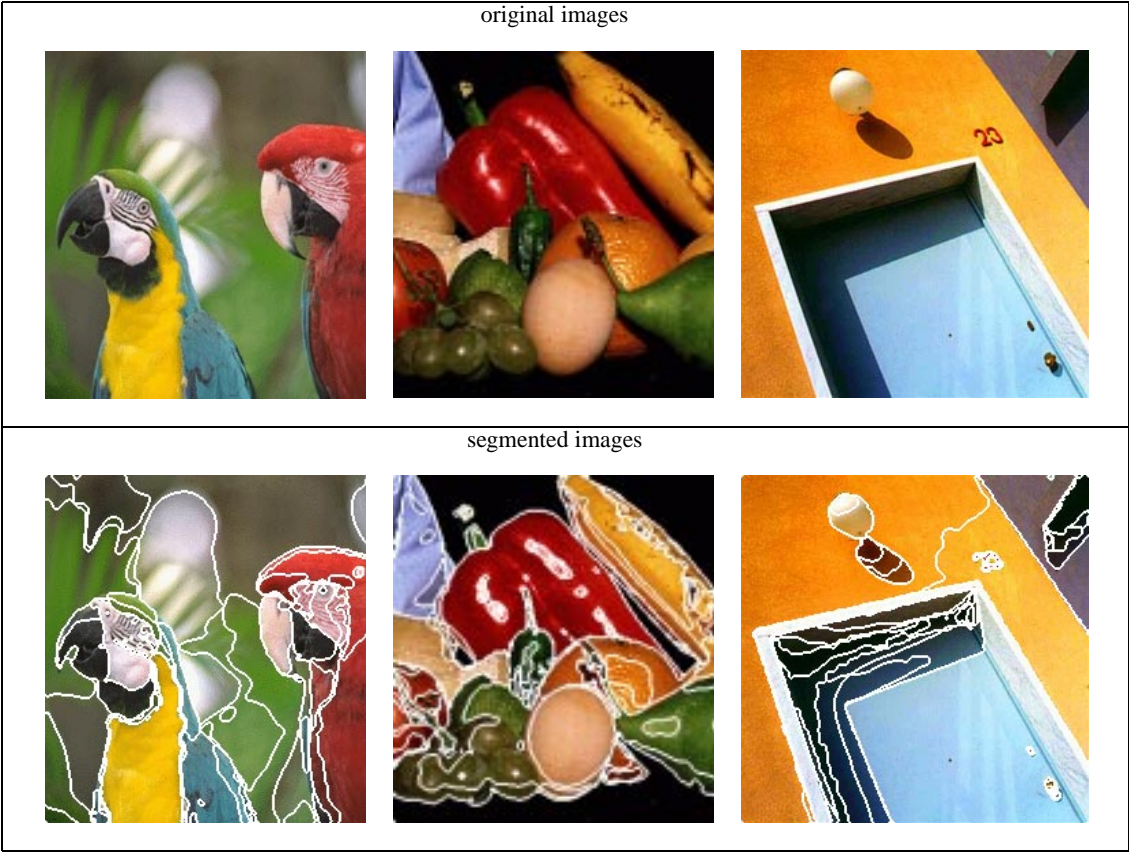


Fig. 2. Some examples of segmentation.